Supplemental Figure Legends

Figure S1 (Related to Figure 1): Different phases of colonic wound healing. (A) Day 1 post-injury (Bar=20 μm) is characterized by loss of crypts and a nascent wound bed. Day 4 post-injury (upper panel, Bar=50 μm) is characterized by squamous wound associated epithelial cells (WAE cells) that cover the denuded surface of the wound. Black arrows indicate WAE cells in the inset (Bar=10 μm). By day 8 post-injury (upper panel, Bar=50μm), WAE cells are replaced by columnar shaped epithelial cells (indicated by red arrows in the inset) and the crypts adjacent to the wound bed formed open extensions (wound channels) that emanate towards the wound bed. The black dashed line indicates a wound channel and black arrows highlight multiple areas of nascent crypts budding from the wound channel (Bar=20 μm). By day 12 post-injury, new crypts have formed and filled in the defect created by the biopsy wound. The black dashed line represents the original wounded area (as determined by the persistent hypertrophy of the muscularis mucosa, Bar=50 μm). See (Manieri et al., 2012; Miyoshi et al., 2012). (B) FITC detected in the serum of mice from the indicated groups post-injury (n=7-10 mice/group). Sham=serum FITC in mice that underwent endoscopy but not biopsy injury. Significance was determined by one-way ANOVA and TUKEY's post hoc test: **$p<0.01$. All values are displayed as mean ± SEM.

Figure S2 (Related to Figure 1): Sustained PGE2 levels impair the transition to wound channel formation and crypt regeneration. (A) Representative images of crypts adjacent to the wound bed 6 days after biopsy injury from vehicle or SW033291-treated mice stained for cleaved caspase-3 (red, apoptotic cells), β-catenin (green, epithelial cells), and bis-benzimide (blue, nuclei). White arrows indicate cells that are caspase-3-positive in the mesenchyme.

Bars=40 μm. (B-D) WT mice were biopsy injured and treated with either vehicle or SW033291 (twice daily from day 4-day 10) and colon tissue distant to the site of injury was evaluated. (B) Representative images of H&E stained sections (Bars=100 μm) at day 12 post-injury from vehicle or SW033291 treated groups. (C) Representative images of crypts distant to the wound bed 12 days after biopsy injury from the indicated groups stained for Ki-67 (red, proliferating cells), β-catenin (green, epithelial cells), and bis-benzimide (blue, nuclei). Bars=40 μm. (D) Quantification of Ki-67 positive epithelial cells from mice in (C) (n=11-12 wounds/group from 4-5 mice/group). (E-F) WT mice were biopsy injured and treated with either vehicle, dmPGE2, or the PGI2 analog Iloprost (twice daily from day 4-day 10). (E) Quantification of Ki-67-positive epithelial cells at day 6 post-injury (n=13-16 wounds/group from 5-6 mice/group). Significance was determined by one-way ANOVA and TUKEY's post hoc test: **p<0.01 (F) Representative images of H&E stained wound sections at day 12 post-injury from the indicated groups. Bars=100 μm. The black line at the center of the wounds indicates wound bed length. All values in D and E are displayed as mean ± SEM.

Figure S3 (Related to Figure 2): TLR2 is required for PGE2 induction during the barrier re-establishment phase of wound repair. (A-C) WT cMSCs were cultured, treated with the indicated TLR agonists at four different concentrations (1, 10,100 and 1000 ng/ml). Levels of PGE2 in the 24-hour culture supernatants from cMSCs treated with (A) Pam3CSK4, (B) Pam2CSK4 or (C) LPS. Significance was determined by one-way ANOVA and TUKEY's post hoc test: **p<0.01, ***p<0.001, ****p<0.0001. (D) cMSCs from WT and *TLR2*$^{-/-}$ mice were cultured and treated with Pam3CSK4 (Pam3) or vehicle. PGE2 was measured in the 24-hour culture supernatants (n=3 experiments). Significance was determined by one-way ANOVA and TUKEY's post hoc test: ****p<0.0001, ns=not significant. (E-G) WT and *TLR2*$^{-/-}$ mice were

biopsy injured and healing was evaluated. (E) Wound tissue was collected at day 4 post-injury for measurement of PGE2 levels by ELISA of the homogenates (n=16-19 wounds/group from 5-6 mice/group). Significance was determined by unpaired Student's t test: **p<0.01. (F) Representative images of wound sections from WT and *TLR2*$^{-/-}$ mice at day 4 post injury stained for claudin-4 (red, WAE cells) and bis-benzimide (blue, nuclei). Bars=100µm. White arrows denote WAE cells, asterisk represents wound bed and the adjacent crypts are indicated by white dashed lines. (G) Quantification of wound repair (based on imaging of whole mounts) of the indicated groups (n= 8-18 wounds per group from 3-7 mice per group). Significance was determined by unpaired Student's t test: ***p<0.001. (H) After collecting the 24-hour culture supernatants from the secondary screen 96 well plate, cells were washed with PBS and incubated with MTT reagent to assess cell survival (n=3 experiments). DCA treatment did not alter cell viability at any of the doses tested as compared to m-toluic acid (100µM) and spermidine (100µM). (I) cMSCs were stimulated with the indicated agonists for 24 hours and subsequently washed in PBS and lysed. The lysates were analyzed for PGE2 levels by ELISA (n=3 independent experiments). Significance was determined by one-way ANOVA and TUKEY's post hoc test: **p<0.01. All values in A-F and G-I are displayed as mean ± SEM.

Figure S4 (Related to Figure 3): Vancomycin mediated reduction of DCA levels and inhibition of crypt regeneration is reversed by blocking PGE2 synthesis. (A) WT colonic mucosal tissue distant to the wound site was collected on day 4 post-injury and analyzed for DCA levels by mass spectrometry (n=9-11 wounds/ group from 3 mice per group). Sham=colonic tissue from mice that underwent endoscopy but not biopsy injury. (B-C) Mice were treated with either vancomycin or vehicle starting 2 weeks prior to biopsy injury and the treatment continued until the day of sacrifice as shown in Figure 3B. (B) Fecal DCA

concentrations determined by mass spectrometry at day 6 post-injury from vehicle and vancomycin treated mice (n=16-33 wounds/group from 6-10 mice/group). Significance was determined by Mann Whitney test: ****p<0.0001. (C) Quantification of Ki-67 positive epithelial cells at day 6 post-injury in vehicle and vancomycin-treated mice (n=14-15 wounds/group from 5 mice/group). Significance was determined by unpaired Student's t test: ****p<0.0001. (D) Vancomycin treated mice were injured, treated with either vehicle or NS-398 and wound PGE2 levels were measured by ELISA at day 6 post-injury (n=13- 17 wounds/group from 5-6 mice/group). Significance was determined by unpaired Student's t test: ***p<0.001. All values are displayed as mean ± SEM.

Figure S5 (Related to Figure 4): DCA reconstitution reversed vancomycin phenotype. (A-B) Vancomycin-treated mice were injured and then intrarectally administered DCA (100 µM, twice daily from day 4-day 10) or equivalent volumes of vehicle as shown in Figure 4A. (A) Plot of Ki-67 positive epithelial cells per wound at day 6 post-injury (n=10-11 wounds/group from 4-5 mice/group). Significance was determined by unpaired Student's t test: *p<0.05. (B) Representative images of wound sections at day 6 post-injury that were stained for cleaved caspase-3 (red, apoptotic cells), β-catenin (green, epithelial cells), and bis-benzimide (blue, nuclei). Dashed white line indicates wound adjacent crypts and asterisks indicate wound beds. The upper panel was a wounded area and the lower panel was an area ~10 crypts away from the wounded region. The White arrow indicates a capase-3 positive cell. Bars=40 µM. (C-E) Vancomycin-treated mice were biopsy injured and administered either DCA (100 µM, twice daily from day 0-day 3) or an equivalent volume of vehicle. Mice were sacrificed on day 4 post-injury and wounds were collected for whole mount analysis and PGE2 production. (C) Representative whole mount images of wounds from indicated groups of mice. Bars= 200µm.

The original wounded area is outlined with white dashed lines and the asterisk indicates a fibrin cap. (D) Quantification of wound healing at day 4 post-injury in the indicated groups (n= 10-11 wounds per group from 4 mice per group). Significance was determined by unpaired Student's t test: ****p<0.0001. (E) Wound PGE2 levels measured in indicated groups of mice (n=11-13 wounds/group from 5 mice/group). Significance was determined by unpaired Student's t test: *p<0.05. (F-G) Vancomycin pre-treated mice were biopsy injured and gavaged twice with PBS, *C. scindens* or *C. clostridioforme* as shown in Figure 4E. (F) Stool from the gavaged groups was collected at day 6 post-injury and genomic DNA was isolated. Colonization was confirmed by PCR based detection of specific bacterial genes. baiCD corresponds to the bile acid inducible gene found in *C. scindens* and rpoB is RNA polymerase beta-subunit gene (see methods for primer details). Each number corresponded to a single mouse. (G) Wound DCA levels at day 6 post-injury in groups of mice described in Figure 5F (n=24-34 wounds/group (from 9-10 mice/group). ND is not detected. Values in A, C, D and G are displayed as mean ± SEM.

Figure S6 (Related to Figure 6): DCA acts via FXR to inhibit cPLA2 expression and PGE2 generation to promote crypt regeneration. (A-D) WT cMSCs were cultured and stimulated with Pam3CSK4 (100ng/ml) in the presence or absence of DCA, INT-777 (TGR5 agonist) or INT-747 (FXR agonist) at the indicated concentrations for 24 hours. Immunoblots of cMSC lysates stained for (A, D) cPLA2, (B) PTGS1, PTGS2, (C) cPGES and mPGES-2. β-Actin was used as the loading control (E) Relative band intensity expressed as fold change over control (n=3 independent experiments). Significance was determined by unpaired Student's t test: *p<0.05. (F-G) Vancomycin pre-treated mice were biopsy injured and intra-rectally administered either CDCA or vehicle (twice daily from day 4-day10 post-injury). (F) Representative images of H&E stained wound sections (Bars=100μm) and (G) wound bed length from indicated groups at

day 12 post-injury (n=9-14 wounds/group from 4-5 mice/group). Significance was determined by unpaired Student's t test: *p<0.05. (H-I) *FXR*$^{-/-}$ mice were injured, treated with either vehicle or NS-398 (twice daily from days 4-10). (H) Representative images of day 12 H&E stained wound sections from *FXR*$^{-/-}$ mice treated with vehicle or NS-398 (PTGS2 inhibitor). (I) Wound bed length from groups of indicated groups of mice (n=16-19 wounds/group from 6 mice/group). Significance was determined by unpaired Student's t test: ***p<0.001. All values in F and H are displayed as mean ± SEM.

Supplemental Table S1 (Related to Figure 2): Screen of microbial metabolites for their effect on Pam3CSK4 induced PGE2 production from cMSCs.

Metabolite number	fold change over Pam3CSK4	Metabolite name
1	1.198315936	3-Phenylpropionic acid
2	0.975084945	valeric acid
3	0.600206453	2'-Deoxycytidine 5'-monophosphate sodium salt
4	1.726265124	p- toluic acid
5	0.80257489	4-Hydroxyphenylacetic acid
6	1.04934347	DL-3-Aminoisobutyric acid
7	0.933264454	N-Methyl-DL-alanine
8	0.706877779	Nα-Acetyl-L-ornithine
9	0.59740957	meso-2,6-Diaminopimelic acid
10	0.771303479	Pyridoxamine dihydrochloride
11	0.795847972	2'-Deoxyadenosine 5'-monophosphate
12	1.501137234	4-Hydroxyindole
13	0.853469256	Oxypurinol
14	1.175569311	Indole-3-acetamide
15	0.541307317	N-Acetyl-L-aspartic acid
16	1.324644414	N-Acetyl-L-glutamic acid
17	1.02612715	N-Acetylneuraminic acid
18	0.956171552	3-Methyl-2-oxobutanoic acid sodium salt
19	1.229726745	DL-Malic acid
20	0.958801012	D-Ribulose 5-phosphate sodium salt
21	0.910403108	D-Pantothenic acid hemicalcium salt

22	0.267239045	4-pyridoxic acid
23	0.672542946	L-Glyceric acid sodium salt
24	1.053824086	α-Ketoglutaric acid
25	0.593489333	Xanthine
26	0.942777355	Cytidine 5'-monophosphate disodium salt
27	0.80802551	4-Methyl-2-oxopentanoic acid sodium salt
28	0.885410638	3-Methyl-2-oxovaleric acid sodium salt
29	1.050120593	3-(4-Hydroxyphenyl)propionic acid
30	1.018299472	γ-Aminobutyric acid
31	1.208131953	L-2-Aminobutyric acid
32	1.535307679	5-Aminovaleric acid
33	0.519237753	L-Homoserine
34	0.798042008	L-Pipecolic acid
35	0.440479753	formate
36	1.349281173	L-Citrulline
37	0.589720037	N-Methyl-L-proline
38	1.20928467	D-Pantothenic acid hemicalcium salt
39	0.880159959	L-Tyrosine methyl ester
40	0.667958345	Piperidine
41	0.905115066	Taurine
42	0.45755904	urea
43	0.955963574	Tyramine
44	1.036369097	Urocanic acid
45	0.838616963	(3-Carboxypropyl)trimethylammonium chloride
46	0.674016905	N-Acetyl-D-glucosamine
47	0.73018728	Nicotinic acid
48	1.11082197	Pyridoxal hydrochloride
49	1.161475763	Pyridoxine
50	1.213872233	Sarcosine
51	1.402429228	N,N-Dimethylglycine
52	1.189336919	Cytosine
53	0.990152094	Uracil
54	0.600444583	Adenine
55	0.645858733	Hypoxanthine
56	0.67883394	Guanine
57	0.821188825	Cytidine
58	0.89762589	Cytidine 2':3'-cyclic monophosphate monosodium salt
59	1.171135969	D-Ala-D-Ala
60	0.842890857	1,3-Diaminopropane
61	0.953958811	Amino-2-propanol
62	0.424357137	deoxycholic acid

63	0.538790402	L-Methionine
64	0.798151084	Putrescine
65	0.693165161	Cadaverine
66	0.805983933	Glutaric acid
67	0.364868343	deoxycholate
68	0.878665279	5-Hydroxyindole-3-acetic acid
69	0.878114711	dTMP
70	1.010822938	Saccharopine
71	0.859951031	Ornithine
72	0.984427794	Beta-alanine
73	0.958495672	dmPGE2
74	0.786514848	butyric acid
75	0.114641017	spermidine
76	0.883956378	fumaric acid
77	0.869800064	succinic acid
78	0.727013506	propionate
79	0.8061	Lactic acid
80	0.488744103	m-toluic acid
81	0.85621392	Isobutyric acid
82	1.164780118	butyrate
83	0.682375917	lithocholic acid
84	0.703422303	acetate

Figure S1

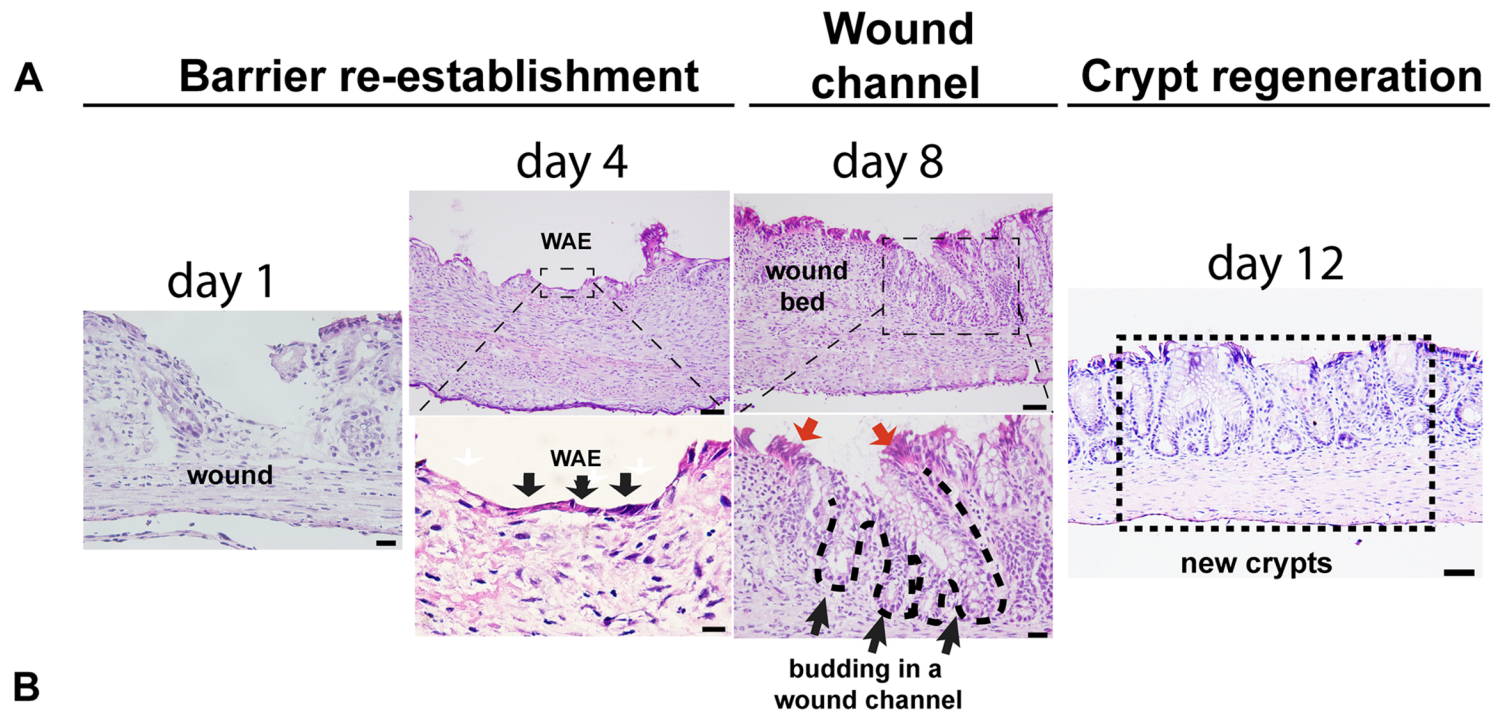
A
Barrier re-establishment
Wound channel
Crypt regeneration
day 1
day 4
day 8
day 12
WAE
WAE
wound
wound bed
new crypts
budding in a wound channel

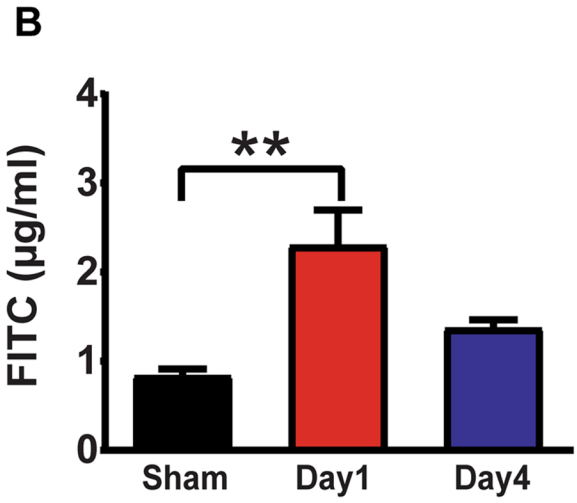
B
FITC (µg/ml)
4
3
2
1
0
**
Sham
Day1
Day4

Figure S2

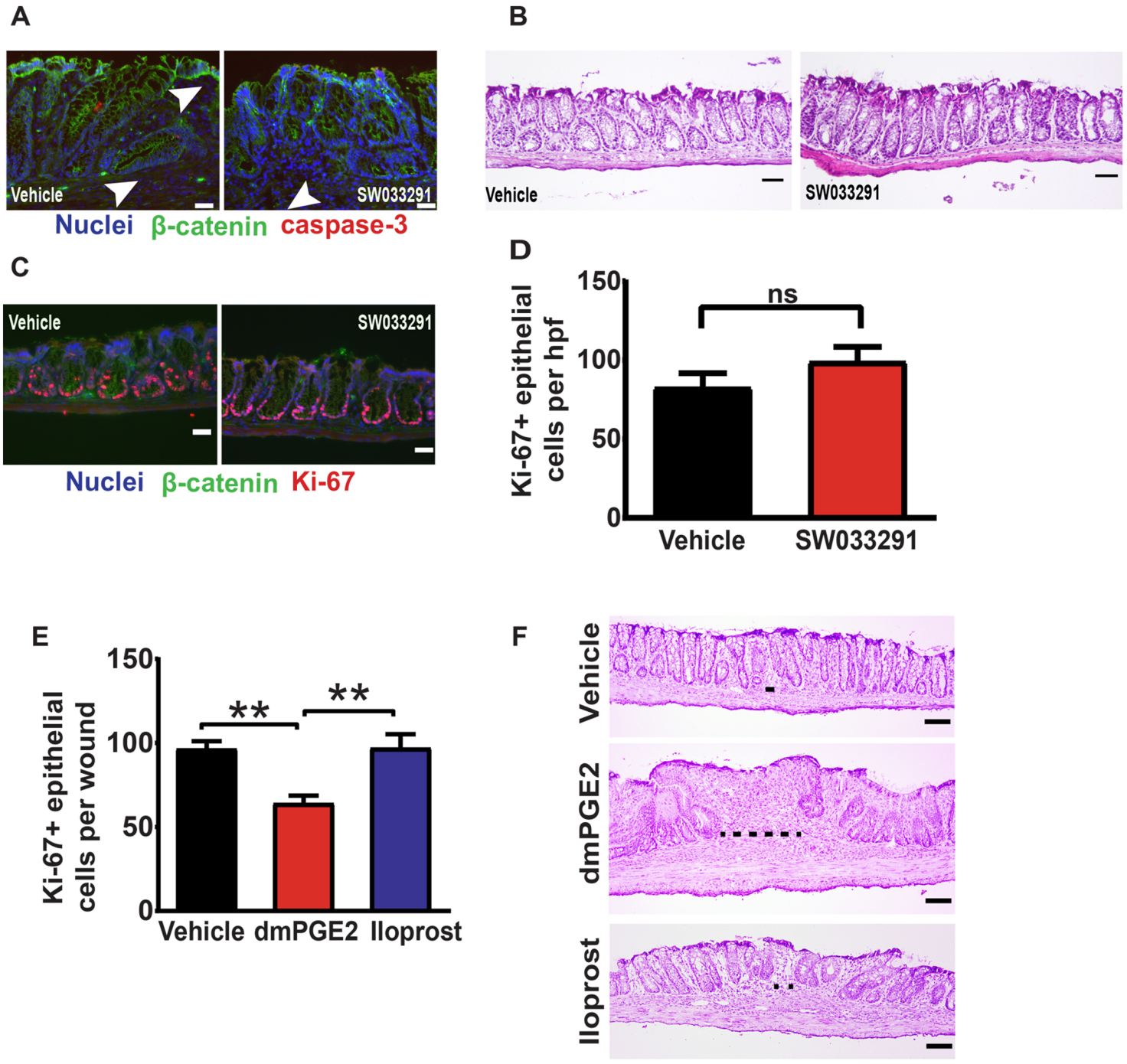
A
Vehicle
SW033291
Nuclei β-catenin caspase-3
B
Vehicle
SW033291
C
Vehicle
SW033291
Nuclei β-catenin Ki-67
D
Ki-67+ epithelial cells per hpf
150
100
50
0
ns
Vehicle
SW033291
E
Ki-67+ epithelial cells per wound
150
100
50
0
**
**
Vehicle dmPGE2 Iloprost
F
Vehicle
dmPGE2
Iloprost

Figure S3

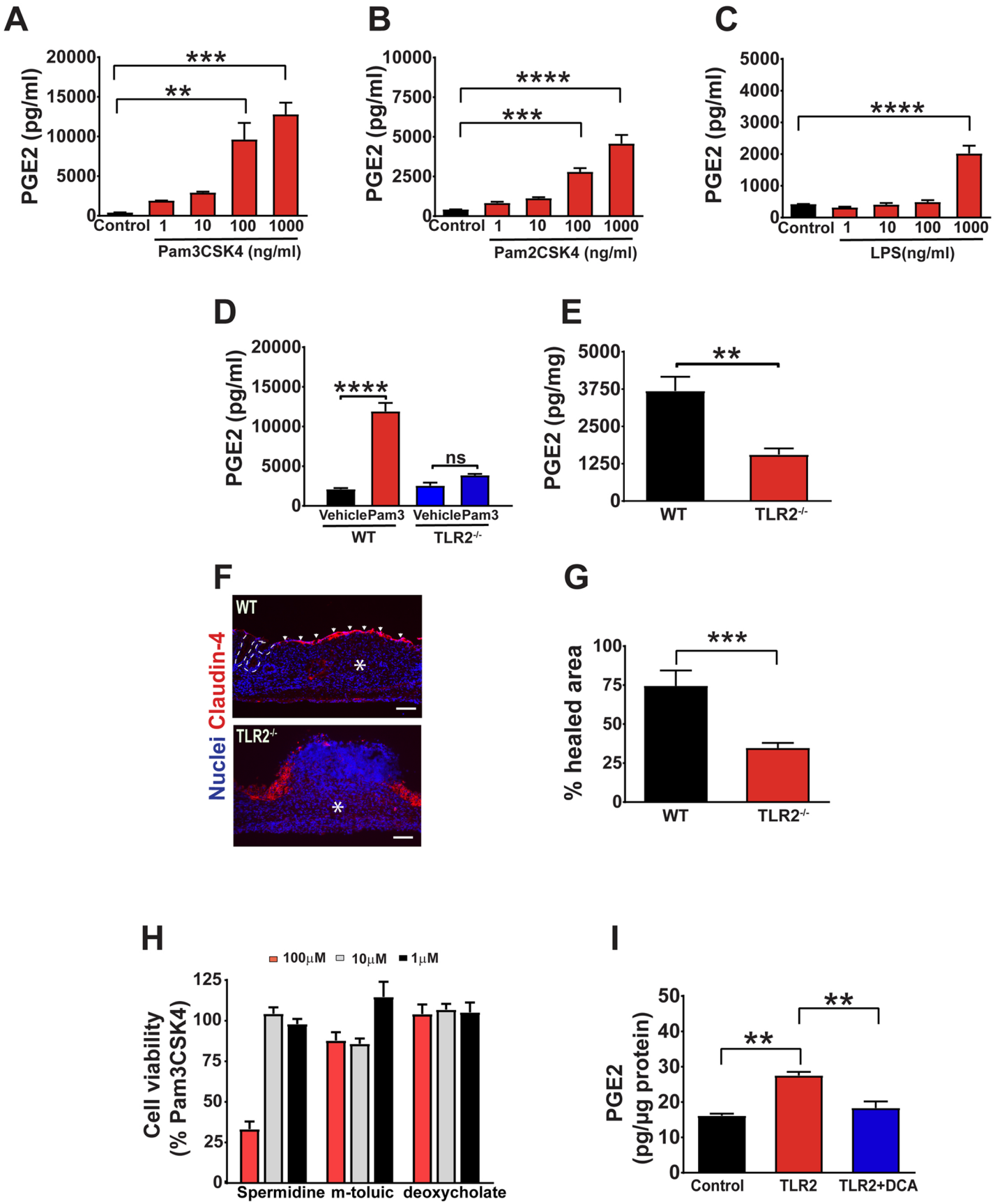
A
PGE2 (pg/ml)
20000
15000
10000
5000
0
***
**
Control 1 10 100 1000
Pam3CSK4 (ng/ml)
B
PGE2 (pg/ml)
10000
7500
5000
2500
0
****
***
Control 1 10 100 1000
Pam2CSK4 (ng/ml)
C
PGE2 (pg/ml)
5000
4000
3000
2000
1000
0
****
Control 1 10 100 1000
LPS(ng/ml)
D
PGE2 (pg/ml)
20000
15000
10000
5000
0
****
ns
Vehicle Pam3 Vehicle Pam3
WT
TLR2-/-
E
PGE2 (pg/mg)
5000
3750
2500
1250
0
**
WT
TLR2-/-
F
Nuclei Claudin-4
WT
TLR2-/-
G
% healed area
100
75
50
25
0
***
WT
TLR2-/-
H
100μM 10μM 1μM
Cell viability (% Pam3CSK4)
125
100
75
50
25
0
Spermidine m-toluic deoxycholate
I
PGE2 (pg/μg protein)
50
40
30
20
10
0
**
**
Control TLR2 TLR2+DCA

Figure S4

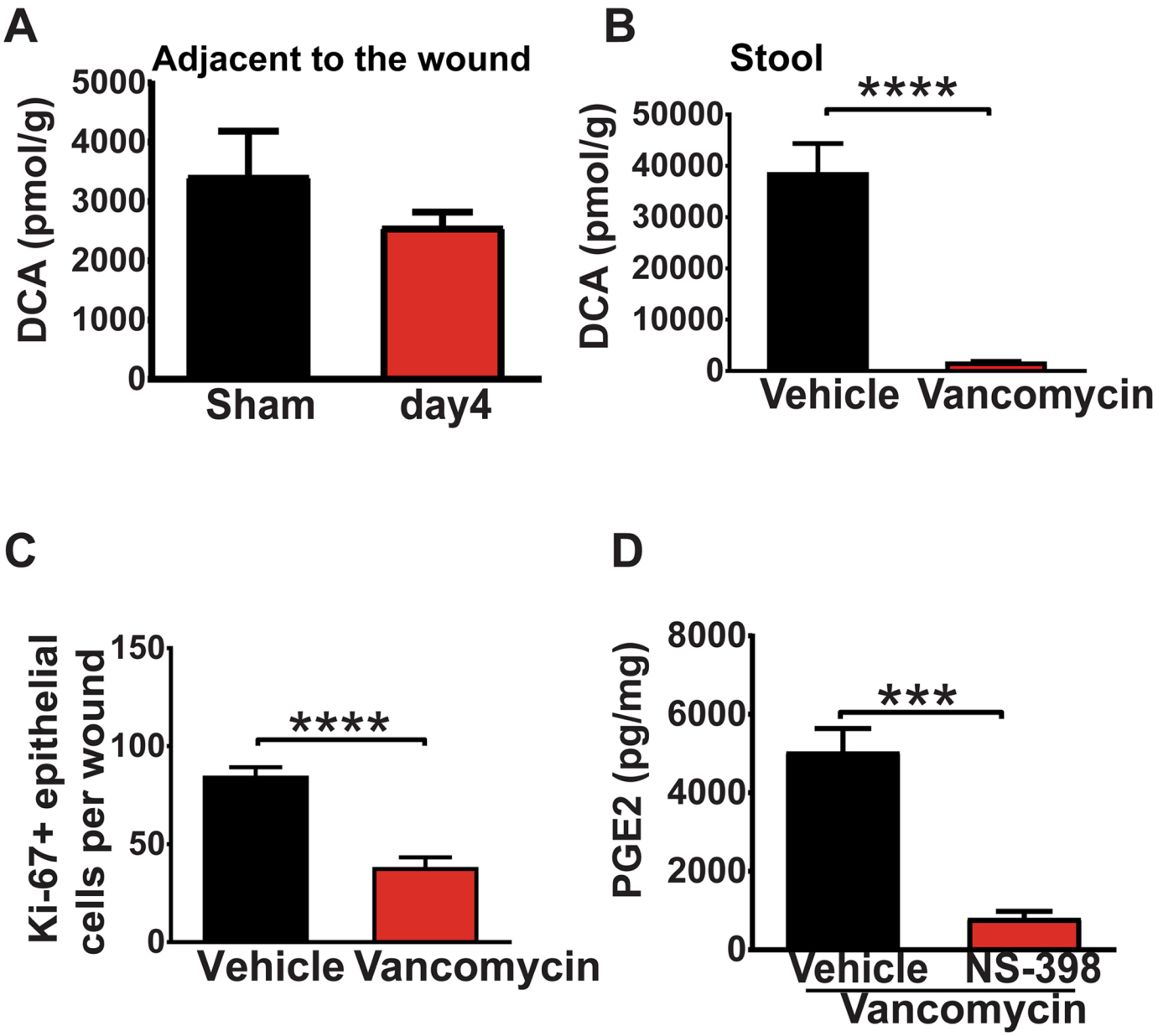
A
Adjacent to the wound
DCA (pmol/g)
5000
4000
3000
2000
1000
0
Sham
day4
B
Stool
****
DCA (pmol/g)
50000
40000
30000
20000
10000
0
Vehicle
Vancomycin
C
Ki-67+ epithelial cells per wound
150
100
50
0
****
Vehicle
Vancomycin
D
PGE2 (pg/mg)
8000
6000
4000
2000
0
***
Vehicle
NS-398
Vancomycin

Figure S5

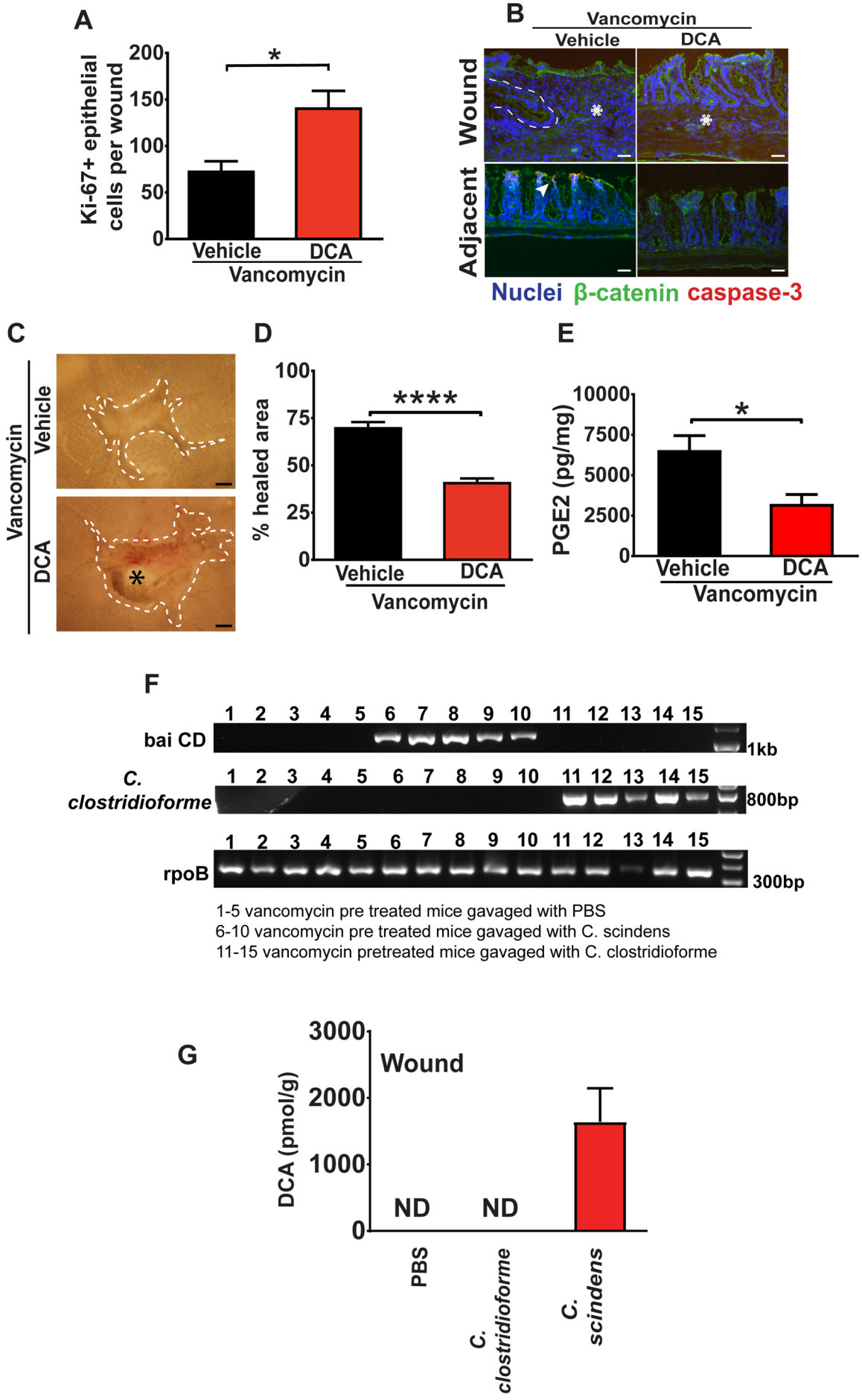
A
Ki-67+ epithelial cells per wound
200
150
100
50
0
*
Vehicle
DCA
Vancomycin
B
Vancomycin
Vehicle
DCA
Wound
Adjacent
Nuclei β-catenin caspase-3
C
Vancomycin
Vehicle
DCA
*
D
% healed area
100
75
50
25
0
****
Vehicle
DCA
Vancomycin
E
PGE2 (pg/mg)
10000
7500
5000
2500
0
*
Vehicle
DCA
Vancomycin
F
1 2 3 4 5 6 7 8 9 10 11 12 13 14 15
bai CD
1kb
C. clostridioforme
800bp
rpoB
300bp
1-5 vancomycin pre treated mice gavaged with PBS
6-10 vancomycin pre treated mice gavaged with C. scindens
11-15 vancomycin pretreated mice gavaged with C. clostridioforme
G
DCA (pmol/g)
3000
2000
1000
0
Wound
ND
ND
PBS
C. clostridioforme
C. scindens

Figure S6

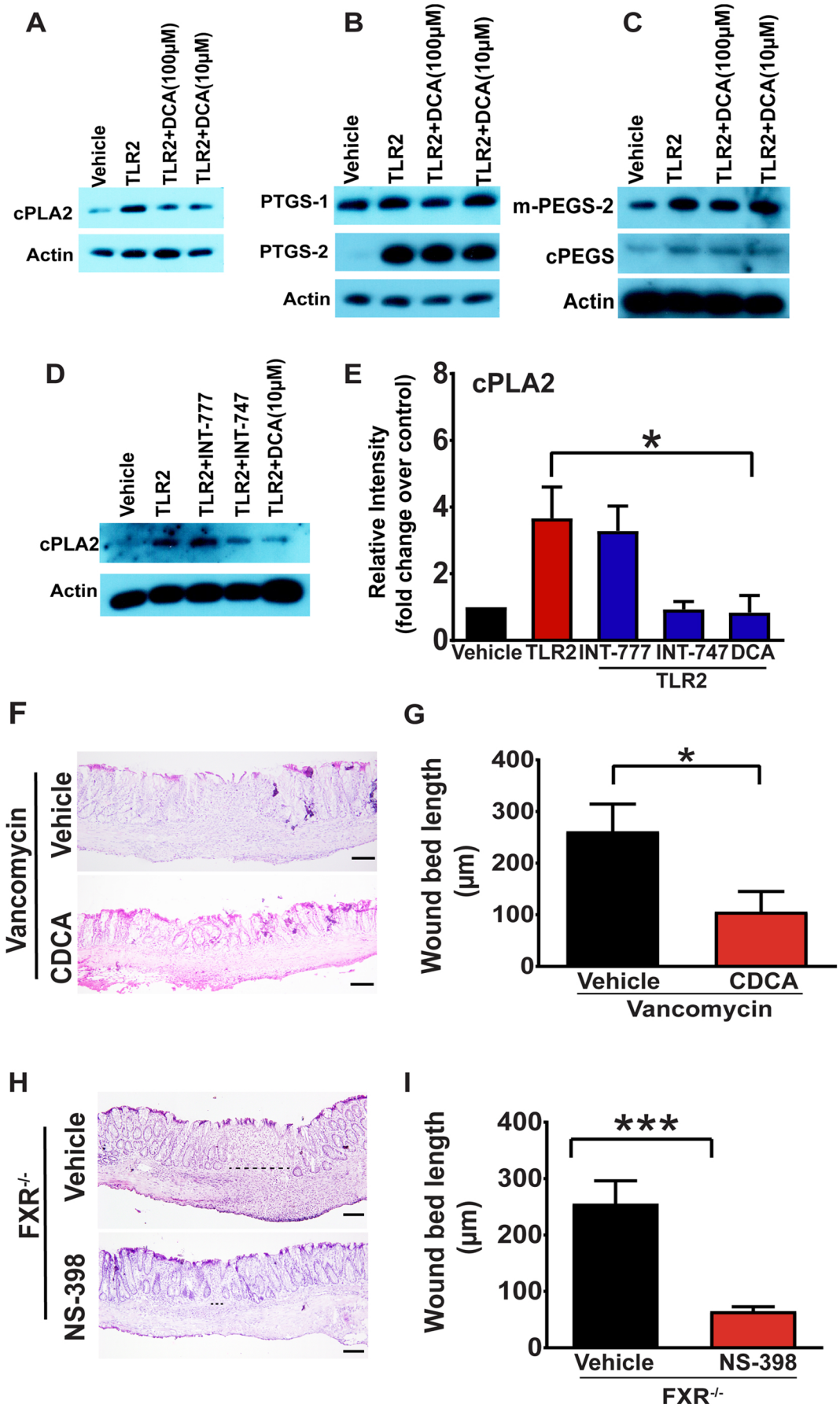
A
Vehicle
TLR2
TLR2+DCA(100μM)
TLR2+DCA(10μM)
cPLA2
Actin
B
PTGS-1
PTGS-2
Actin
C
m-PEGS-2
cPEGS
Actin
D
TLR2+INT-777
TLR2+INT-747
TLR2+DCA(10μM)
E
cPLA2
Relative Intensity
(fold change over control)
Vehicle
TLR2
INT-777
INT-747
DCA
TLR2
F
Vancomycin
Vehicle
CDCA
G
Wound bed length
(μm)
Vehicle
CDCA
Vancomycin
H
FXR-/-
Vehicle
NS-398
I
Wound bed length
(μm)
Vehicle
NS-398
FXR-/-